

Structures of photochemically prepared mixed-valence polyoxovanadate clusters: oblong $[\text{V}_{18}\text{O}_{44}(\text{N}_3)]^{14-}$, superkeggin $[\text{V}_{18}\text{O}_{42}(\text{PO}_4)]^{11-}$ and doughnut-shaped $[\text{V}_{12}\text{B}_{32}\text{O}_{84}\text{Na}_4]^{15-}$ anions†

Toshihiro Yamase,* Masamichi Suzuki and Kawori Ohtaka

Research Laboratory of Resources Utilization, Tokyo Institute of Technology, 4259 Nagatsuta, Midori-ku, Yokohama 226, Japan

Three mixed-valence polyoxovanadates, $\text{Na}_{12}\text{H}_2[\text{V}_{18}\text{O}_{44}(\text{N}_3)] \cdot 30\text{H}_2\text{O}$ **1**, $\text{K}_{8.5}\text{H}_{2.5}[\text{V}_{18}\text{O}_{42}(\text{PO}_4)] \cdot 19\text{H}_2\text{O}$ **2** and $\text{H}_{15}[\text{V}_{12}\text{B}_{32}\text{O}_{84}\text{Na}_4] \cdot 13\text{H}_2\text{O}$ **3** have been photochemically synthesized and characterized by X-ray single-crystal analysis and magnetic susceptibility measurements. The $[\text{V}_{18}\text{O}_{44}(\text{N}_3)]^{14-}$ anion has an oblong structure encapsulating a linear N_3^- anion with approximate D_{2h} symmetry. The extent of reduction is different from that in $[\text{V}_{18}\text{O}_{44}(\text{N}_3)]^{7-}$ prepared by thermal decomposition of $[\text{V}_{19}\text{O}_{50}]^{17-}$ in the presence of N_3^- at 75 °C. The $[\text{V}_{18}\text{O}_{42}(\text{PO}_4)]^{11-}$ anion has a superkeggin structure with a $\text{PV}_{12}\text{O}_{40}$ Keggin unit capped by six VO moieties which lie above six rectangle faces of the T_d -distorted cuboctahedron defined by the V atoms in the Keggin unit. The $[\text{V}_{12}\text{B}_{32}\text{O}_{84}\text{Na}_4]^{15-}$ anion contains an edge-sharing dodecagonal array of OVO_4 square pyramids, sandwiched by two hexadecaborates to produce a cyclic doughnut-shaped framework. The crystallographic analysis indicates that the cavity produced by the cyclic $[\text{V}_{12}\text{B}_{32}\text{O}_{84}]^{19-}$ anion is occupied by a tetragonal Na_4^{4+} moiety. The paramagnetic complexes **1–3** show the antiferromagnetic exchange interaction which is discussed in terms of the nearest $\text{V} \cdots \text{V}$ distances in the anion.

In the course of our studies on the photochemical control of the structural variety of the polyoxovanadate clusters which serve as hosts for neutral and charged species with vastly different cavity requirements, structures of the spherical isopolyoxovanadates $[\text{V}_{15}\text{O}_{36}(\text{CO}_3)]^{7-}$, $[\text{H}_{3.5}\text{V}_{18}\text{O}_{42}\text{Cl}]^{9.5-}$ and $[\text{H}_2\text{V}_{18}\text{O}_{42}(\text{H}_2\text{O})]^{10-}$ have been reported.^{1,2} In this type of photochemical assembly, the reaction of aqueous solutions containing $[\text{V}_4\text{O}_{12}]^{4-}$ and alcohols as electron donors in the presence of a variety of charged species is triggered by electron transfer from the alcohol to the $\text{O} \rightarrow \text{V}$ ligand-to-metal charge-transfer (l.m.c.t.) excited triplet states. Although the mechanistic details of the preferential formation of encapsulating polyoxovanadates are not always clear, the structure of the spherical polyoxovanadate shells strongly depends on the structure of the capsulated species (templates) and solution pH.^{3,4} To extend the scope of the photoinduced self-recognition to other templates, we have investigated the photochemical formation of both V_{18} clusters $[\text{V}_{18}\text{O}_{44}(\text{N}_3)]^{14-}$ and $[\text{V}_{18}\text{O}_{42}(\text{PO}_4)]^{11-}$ and a $\text{V}_{12}/\text{B}_{32}$ mixed cluster of $[\text{V}_{12}\text{B}_{32}\text{O}_{84}\text{Na}_4]^{15-}$. The N_3^- -encapsulated V_{18} anion has been also reported for $[\text{V}_{18}\text{O}_{44}(\text{N}_3)]^{7-}$ produced by the thermal decomposition of $[\text{V}_{19}\text{O}_{50}]^{17-}$ in the presence of N_3^- at 75 °C.⁵ However, unlike the photolysis product, the number (eight) of vanadium(IV) ions in the anion was small. Such a difference between the two anions indicates that anions offer many opportunities for the isomerism of mixed-valence states which depend on the preparation method. The $[\text{V}_{18}\text{O}_{42}(\text{PO}_4)]^{11-}$ anion exhibits the superkeggin structure observed for the $[\text{V}_{18}\text{O}_{42}(\text{VO}_4)]^{15-}$ and $[\text{V}_{18}\text{O}_{42}(\text{SO}_4)]^{8-}$ anions.⁶ The $[\text{V}_{12}\text{B}_{32}\text{O}_{84}\text{Na}_4]^{15-}$ anion is the first example of a cyclic belt-shaped dodecavanadate sandwiched by hexadecaborates with a plausible location of the Na_4^{4+} tetragonal moiety in the central cavity. There have been only a few examples of alkali-metal cation-encapsulated polyoxometalates (polyoxotungstates, so far): $[\text{Sb}_9\text{W}_{21}\text{O}_{86}\text{Na}]^{18-}$,⁷ $[\text{As}_4\text{W}_{40}\text{O}_{140}\text{K}]^{27-}$,⁸ $[\text{W}_{18}\text{O}_{56}(\text{HF}_3)_2\text{Na}]^{7-9}$ and $[\text{P}_5\text{W}_{30}\text{O}_{110}\text{Na}]^{14-}$.¹⁰ As part of our effort to identify photochemical encapsulation materials and to clarify their structural

chemistry, we report here the structures of $\text{Na}_{12}\text{H}_2[\text{V}_{18}\text{O}_{44}(\text{N}_3)] \cdot 30\text{H}_2\text{O}$ **1**, $\text{K}_{8.5}\text{H}_{2.5}[\text{V}_{18}\text{O}_{42}(\text{PO}_4)] \cdot 19\text{H}_2\text{O}$ **2** and $\text{H}_{15}[\text{V}_{12}\text{B}_{32}\text{O}_{84}\text{Na}_4] \cdot 13\text{H}_2\text{O}$ **3**. Such general features are important for the photochemical design of nano composites.

Experimental

Preparation and chemical analysis

All the reagents were of at least analytical grade and used without further purification. The salt $[\text{NH}_3\text{Bu}^+]_4[\text{V}_4\text{O}_{12}]$ was synthesized according to the published procedure and identified in the solid state by comparison of the IR spectrum with that previously reported.¹¹ The cluster $\text{Na}_{12}\text{H}_2[\text{V}_{18}\text{O}_{44}(\text{N}_3)] \cdot 30\text{H}_2\text{O}$ **1** was prepared as follows: an aqueous solution (pH 7.6) containing $[\text{NH}_3\text{Bu}^+]_4[\text{V}_4\text{O}_{12}]$ (0.4 g, 0.6 mmol) and NaN_3 (0.8 g, 12 mmol) in water (20 cm³) in a Pyrex tube (20 cm³) was adjusted to pH 9.4 with KOH and MeOH (2 cm³) was added. The resulting solution was irradiated for 6.5 h under an atmosphere of nitrogen using a 500 W superhigh-pressure mercury lamp. Dark brown single rhombic crystals were precipitated within 1 d with a yield of 0.1 g. The cluster $\text{K}_{8.5}\text{H}_{2.5}[\text{V}_{18}\text{O}_{42}(\text{PO}_4)] \cdot 19\text{H}_2\text{O}$ **2** was prepared similarly: an aqueous solution (20 cm³) containing $[\text{NH}_3\text{Bu}^+]_4[\text{V}_4\text{O}_{12}]$ (0.4 g, 0.6 mmol) and KH_2PO_4 (0.25 g, 1.8 mmol) was adjusted to pH 9.4 with KOH, and MeOH (2 cm³) was added. Photolysis of the resulting solution for 18 h provided dark brown single rhombic crystals with a yield of 0.2 g. The cluster $\text{H}_{15}[\text{V}_{12}\text{B}_{32}\text{O}_{84}\text{Na}_4] \cdot 13\text{H}_2\text{O}$ **3** was prepared as follows: an aqueous solution (20 cm³) containing Na_3VO_4 (1.0 g, 5.5 mmol) was adjusted to pH 7.0 with H_3BO_3 (28 g, 45.3 mmol) and then MeOH (2 cm³) was added. Photolysis of the resulting solution for 3 d provided green single hexagonal crystals with a yield of 0.3 g. Crystalline **3** was also prepared by using $[\text{NH}_3\text{Bu}^+]_4[\text{V}_4\text{O}_{12}]$ instead of Na_3VO_4 . A part of the sodium cations for **3** is accessible to exchange to trivalent lanthanide cation by mixing **3** with $\text{Ln}(\text{NO}_3)_3$ in water. Other cation (Li^+ or K^+)-containing dodecavanadodotriacontaborates were synthesized by the modified procedure and identified by comparison of the IR spectra with **3**: an aqueous solution (at pH 12) containing $[\text{NH}_3\text{Bu}^+]_4[\text{V}_4\text{O}_{12}]$ (0.5 g, 0.7 mmol) and

† Photochemistry of polyoxovanadates. Part 3.^{1,2}

Non-SI units employed: $\mu_B \approx 9.27 \times 10^{-24} \text{ J T}^{-1}$; $\text{emu} = 4\pi \times 10^{-6} \text{ m}^3$.

LiOH (0.22 g, 7.6 mmol) was adjusted to pH 7.0 with H_3BO_3 (2.5 g, 40.4 mmol) and MeOH (2 cm³) was added. The resulting solution was irradiated for 3 d. The concentrated photolyte provided green hexagonal crystals after 1–2 weeks with a yield of 0.1 g.

The vanadium content of compounds **1–3** was determined using the potentiometric method by detecting the end-points of titrations with Fe^{2+} (for V^{V}) and Mn^{VII} (for V^{IV}) in stirred H_2SO_4 solutions. Measurements of the potential using a platinum indicator electrode vs. a Ag–AgCl reference electrode at open circuit were carried out using a TOA Electronics IM-5S ion meter. The number of vanadium(IV) centres was unambiguously established by back titration analysis for **1–3**: a known excess of ammonium iron(II) sulfate was added to the sample in 1 mol dm^{−3} H_2SO_4 to reduce V^{V} to V^{IV} which was determined using a standard solution of KMnO_4 . The vanadium(IV) content for **3** was also potentiometrically determined using a standard solution of $[\text{NH}_4]_2[\text{Ce}(\text{NO}_3)_6]$. The potentiometric titrations of **1–3** gave fifteen (15 ± 0.4), fourteen (14 ± 0.5) and seven (7 ± 0.2) electron reductions per anion respectively, which correspond to the numbers of vanadium(IV) centres in the anions. Sodium and potassium were determined potentiometrically by use of a TOA Electronics IM-5S ion meter. Phosphorus analysis was carried out on an X-ray-fluorescence element analyser (JEOL, JSX-3200). Thermogravimetric analysis using a Rigaku Thermoflex TG-DGC instrument was used for the determination of lattice water (Found: N, 1.95; Na, 12.0; V, 36.95. Calc. for $\text{H}_{62}\text{N}_3\text{Na}_{12}\text{O}_{74}\text{V}_{18}$: N, 1.7; Na, 11.1; V, 36.95. Found: K, 14.95; P, 1.3; V, 39.6. Calc. for $\text{H}_{40.5}\text{K}_{8.5}\text{O}_{65}\text{PV}_{18}$: K, 14.1; P, 1.3; V, 38.85. Found: Na, 4.05; V, 22.55. Calc. for $\text{B}_{32}\text{H}_{41}\text{Na}_4\text{O}_{97}\text{V}_{12}$: Na, 3.5; V, 23.15%). Infrared spectra were recorded on a JASCO FT/IR-5000 spectrometer. The magnetic measurements were carried out on microcrystalline samples with a magnetometer (Quantum design, MPMS-5S) equipped with a SQUID sensor. The temperature range was 4–300 K and the magnetic field was 1.0 T. The molar susceptibility was corrected for the diamagnetic contributions of clusters **1–3** (-1065×10^{-6} , -1006×10^{-6} and -1310×10^{-6} emu mol^{−1}, respectively) using standard Pascal constants.¹²

Crystallography

Crystals of compounds **1–3** were sealed in Lindemann glass capillaries and mounted on a Rigaku AFC-5S diffractometer equipped with graphite-crystal monochromatized Mo- $\text{K}\alpha$ ($\lambda = 0.71069$ Å) radiation. The intensities were collected by ω -2 θ scans at the 2 θ scan rate of 8° min^{−1} at room temperature. The orientation matrix and cell dimensions were obtained from the setting angles of 25 centred reflections in the ranges 2 $\theta = 20.3$ –25.0, 20.1–24.8 and 20.3–23.9° for **1–3**, respectively. No significant decay of intensity of the three standard reflections recorded after every 100 was observed. The vanadium positions were determined by direct methods using SHELXS 86¹³ for **1** and MITHRIL 90¹⁴ for **2** and **3**. The K, O and B atoms were located from difference syntheses. Lorentz-polarization factors were applied and absorption corrections were made on the basis of ψ scans of three reflections¹⁵ after isotropic refinement for **1** and **2** and by use of DIFABS¹⁶ for **3**. The correction factors applicable to $|F_o|$ were 0.74–1.00, 0.66–1.00 and 0.64–1.31 for **1–3**, respectively. Subsequently for **1** the V, Na and N atoms were refined with anisotropic thermal parameters, for **2** the V, K and P atoms, and for **3** the V, Na and O atoms. Refinements for all non-H atoms were carried out using the full-matrix least-squares method. The quantity minimized was $\sum w(|F_o| - |F_c|)^2$. Attempts to refine sodium, potassium and crystal-water oxygen atoms were made, with various combinations of site occupancy factors. The crystal data for **1–3** are summarized in Table 1. The weighting scheme employed was $w^{-1} = \sigma^2(F_o)$, where $\sigma^2(I_o) = \sigma^2(I_{\text{counting}}) + (0.004I_o)^2$, $\sigma^2(I_{\text{counting}}) + (0.013I_o)^2$, and $\sigma^2(I_{\text{counting}}) + (0.011I_o)^2$ for **1–3**,

respectively. The maximum and minimum heights in the final difference synthesis were 2.2 and -1.2 e Å^{−3} around V(5) and V(9) atoms at distances of 1.0 and 0.5 Å in **1**, 5.6 and -1.3 e Å^{−3} around O(61) and O(13) at 1.4 and 5.3 Å in **2** and 0.8 and -0.6 e Å^{−3} in **3**. All calculations were carried out on a Micro VAX II computer using the TEXSAN software package.¹⁷

The bond strength (s) in valence units was calculated using $s = (d/1.378)^{-4.065}$, $(d/1.791)^{-5.1}$ and $(d/1.770)^{-5.2}$ for the B–O, V^{V} –O and V^{IV} –O bond length (d) in Å, respectively,¹⁸ and the valence sum (bond order = Σs) of all of the B–O, V^{V} –O and V^{IV} –O bond strengths about a given O atom gives the valence of the atom. The alternative expression, $s = \exp[(d_0 - d)/B]$, where d_0 (=1.371, 1.803 and 1.784 Å for B, V^{V} and V^{IV} sites, respectively) and B (=0.37) are empirically determined parameters,¹⁹ gave similar bond-valence values.

Atomic coordinates, thermal parameters, and bond lengths and angles have been deposited at the Cambridge Crystallographic Data Centre (CCDC). See Instructions for Authors, *J. Chem. Soc., Dalton Trans.*, 1997, Issue 1. Any request to the CCDC for this material should quote the full literature citation and the reference number 186/540.

Results and Discussion

Infrared spectra

The IR (KBr disc) spectra of compounds **1–3** are shown in Fig. 1 and exhibit bands around 1630m (1630, 1630 and 1638 for **1–3**, respectively), 950s (959, 944 and 981), 700s (692, 700 and 658) cm^{−1}. The strong broad band at ca. 950 cm^{−1} is due to the terminal V–O stretching of the cluster formed by linking VO_5 and VO_6 polyhedra and the feature at 700–600 cm^{−1} is attributed to symmetric and asymmetric V–O–V stretchings. The strong band at 2016 cm^{−1} for **1** can be assigned to $\nu_{\text{asym}}(\text{NNN})$ stretching mode. Compound **2** exhibits a weak band due to $\nu_{\text{asym}}(\text{P–O})$ at 1050 cm^{−1}. The strong bands around 1330 and 919 cm^{−1} for **3** are due to $\nu_{\text{asym}}(\text{B–O})$ and $\nu_{\text{sym}}(\text{B–O})$ stretchings, respectively.

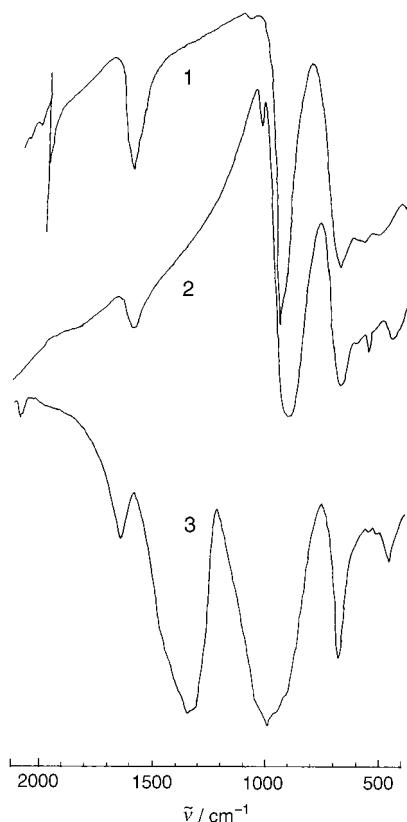
Structures of $\text{Na}_{12}\text{H}_2[\text{V}_{18}\text{O}_{44}(\text{N}_3)] \cdot 30\text{H}_2\text{O}$ **1**, $\text{K}_{8.5}\text{H}_{2.5}[\text{V}_{18}\text{O}_{42}(\text{PO}_4)] \cdot 19\text{H}_2\text{O}$ **2** and $\text{H}_{15}[\text{V}_{12}\text{B}_{32}\text{O}_{84}\text{Na}_4] \cdot 13\text{H}_2\text{O}$ **3**

The unit cells for compounds **1–3** contain one, two and one molecules, respectively. Figs. 2–4 show views of the anion structures. Chemical and X-ray structural analyses of **1–3** formally reveal the presence of twelve Na^+ , eight and half K^+ , and four Na^+ cations for each molecule, respectively. In **1** all of the Na atoms have five to eight contacts to the anion and water O atoms with $\text{Na} \cdots \text{O}$ distances of 2.29(1)–3.04(1) Å. Similarly, in **2** all of the K atoms have four to seven contacts to the anion and water O atoms with $\text{K} \cdots \text{O}$ distances of 2.51(5)–3.09(2) Å. One K atom [K(9)] is disordered with its symmetry equivalent ($1 - x, -y, -z$) in the short distance 1.45(3) Å and was refined with half occupancy. In **3** eight Na atoms at the tetragonal corners with approximate size of $2.62 \times 2.62 \times 2.98$ Å were refined with half occupancies due to disorder, resulting in the location of four Na^+ cations with an approximate tetrahedral arrangement of $\text{Na} \cdots \text{Na}$ distances 3.69(2) and 3.99(2) Å. The Na_4 tetragon is bound to eight oxygen atoms of anion O(20), O(23), O(26), O(29) and their symmetry equivalents ($-x, -y, -z$) in the centre of the doughnut-type anion. Among these connections, eight Na–O distances cover the range 2.61(2)–2.65(2) Å [mean 2.63(1) Å]. It is reasonable to consider that most of the external sodium cations for the polyoxometalates are co-ordinated by more than four oxygen atoms with distances 2.3–3.1 Å, as exemplified by **1**. The possibility of external Na^+ cations for **3** was excluded, since refinement with the full occupancy of eight O atoms at the tetragonal corners provided neither the location of external Na atoms with their reasonable thermal parameters nor co-ordination by a reasonable number of oxygen atoms (at best, only one contact to anion-oxygen atoms with 2.8–3.1 Å).

Table 1 Crystal and refinement data for clusters **1–3***

| | 1 | 2 | 3 |
|---|---|---|---|
| Formula | H ₅₈ N ₃ Na ₁₂ O ₇₂ V ₁₈ | H _{40.5} K _{8.5} O ₆₅ PV ₁₈ | H ₄₁ B ₃₂ Na ₄ O ₉₇ V ₁₂ |
| <i>M</i> | 2445 | 2362 | 2642 |
| Crystal system | Rhombic | Rhombic | Hexagonal |
| <i>a</i> /Å | 12.028(3) | 12.225(3) | 17.344(5) |
| <i>b</i> /Å | 13.127(4) | 12.283(3) | 17.395(5) |
| <i>c</i> /Å | 13.394(3) | 20.833(3) | 17.397(4) |
| <i>α</i> /° | 114.42(2) | 88.79(2) | 75.68(2) |
| <i>β</i> /° | 93.27(2) | 88.75(1) | 60.14(3) |
| <i>γ</i> /° | 113.56(2) | 72.61(1) | 60.12(2) |
| <i>U</i> /Å ³ | 1701(1) | 2984(1) | 3946(2) |
| <i>Z</i> | 1 | 2 | 1 |
| <i>D</i> _c /g cm ^{−3} | 2.422 | 2.627 | 1.120 |
| <i>μ</i> /cm ^{−1} | 25.551 | 34.22 | 7.68 |
| <i>F</i> (000) | 1221 | 2302 | 1292 |
| Crystal size/mm | 0.3 × 0.4 × 0.1 | 0.2 × 0.5 × 0.05 | 0.5 × 0.5 × 0.1 |
| <i>hkl</i> Ranges | ±18, ±18, 0–15 | ±19, ±28, 0–16 | ±23, ±23, 0–23 |
| No. data measured | 8179 | 14 344 | 18 273 |
| No. unique data | 7806 | 13 690 | 18 105 |
| No. observed data | 3491[<i>I</i> > 3.0σ(<i>F</i>)] | 7071[<i>I</i> > 3.0σ(<i>F</i>)] | 5798[<i>I</i> > 4.0σ(<i>F</i>)] |
| No. variables | 298 | 510 | 605 |
| <i>R</i> | 0.076 | 0.084 | 0.093 |
| <i>R</i> ' | 0.074 | 0.093 | 0.101 |
| Goodness of fit, <i>S</i> | 4.97 | 3.77 | 4.82 |
| Maximum shift/error | 0.0008 | 0.0139 | 0.0001 |

* Details in common: space group *P* $\bar{1}$; data collection range 5 ≤ 2θ ≤ 55°.

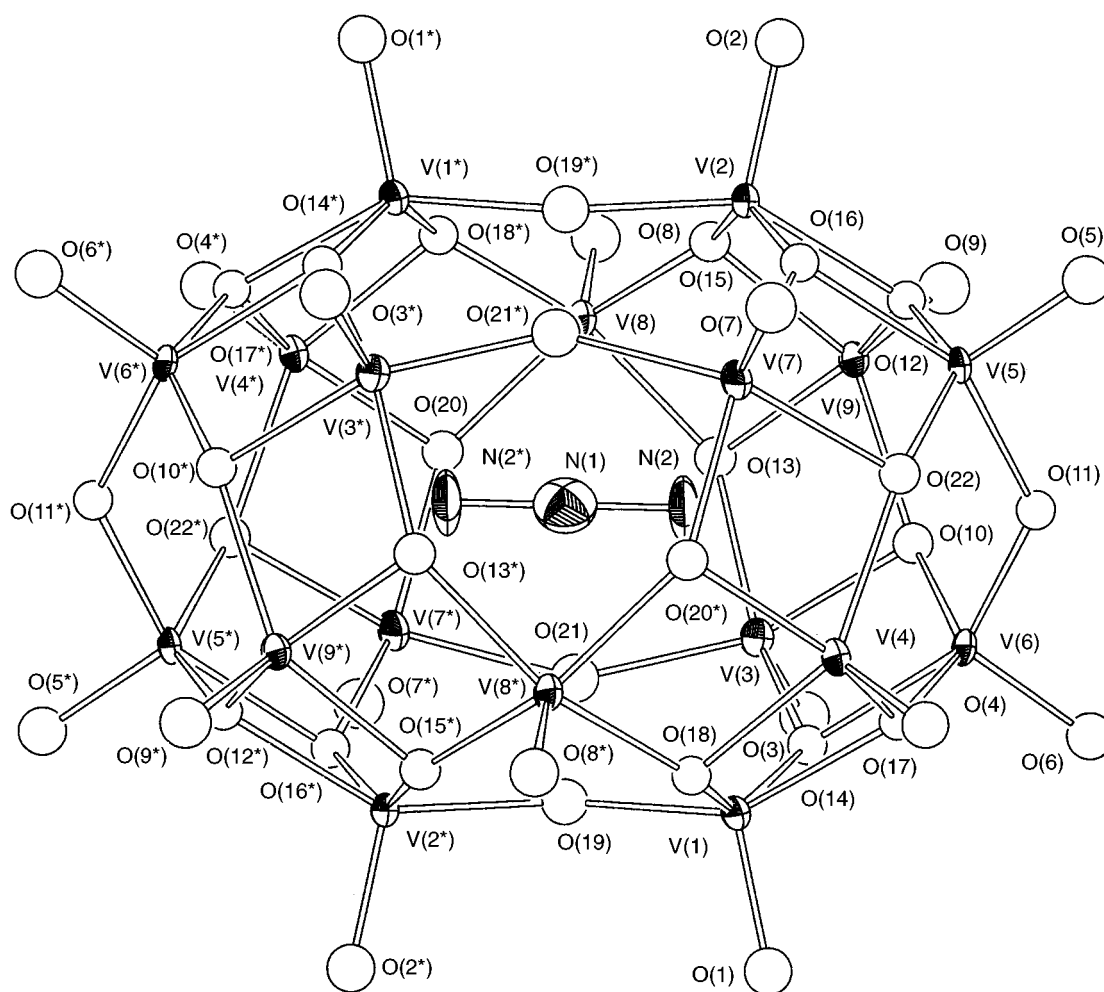
**Fig. 1** Infrared spectra of clusters **1–3**

Each anion of compounds **1–3** is a V^V/V^{IV} mixed-valence compound and formally contains fifteen, fourteen and seven V^{IV}, respectively. Thirty, nineteen and thirteen O atoms of water molecules of crystallization were located for **1–3** respectively and some of them had large thermal parameters due to disorder. Especially, three oxygen atoms O(48), O(49) and O(50) for **3** were refined with half occupancy. Thus, the compositions Na₁₂H₂[V^{IV}₁₅V^V₃O₄₄(N₃)]·30H₂O, K_{8.5}H_{2.5}[V^{IV}₁₄V^V₄O₄₂(PO₄)]·19H₂O and H₁₅[V^{IV}₇V^V₅B₃₂O₈₄Na₄]]·13H₂O, respectively, are necessary to maintain electrical neutrality.

(a) [V^{IV}₁₅V^V₃O₄₄(N₃)]^{14−}. The [V^{IV}₁₅V^V₃O₄₄(N₃)]^{14−} anion in compound **1**, related by a crystallographic inversion centre, has approximate *D*_{2h} symmetry. The anion has an oblong V₁₈O₄₄ cluster shell encapsulating negatively charged N₃[−], which is built up of edge- and corner-sharing OVO₄ square pyramids at neighbouring V...V distances of 2.879(3)–3.022(3) [mean 2.974(2)] and 3.323(3)–3.665(3) Å [mean 3.583(2) Å], respectively. Table 2 shows selected bond distances and angles. The V=O, V–O(μ) and V–O(μ₃) bond distances are 1.608(8)–1.630(8) [mean 1.620(3)], 1.798(7)–1.930(8) [mean 1.855(3)] and 1.877(7)–1.988(7) [mean 1.946(2)] Å, respectively. A simplified vanadium-atom framework of **1** is shown in Fig. 5 where asterisked atoms indicate the symmetry equivalent (−*x*, −2 − *y*, −2 − *z*) atoms. The framework consists of two horizontal rectangle planes V(1,2*,7*,3) and V(1*,2,7,3*), one horizontal hexagon plane V(4,8*,9*,4*,8,9) and one vertical rectangle plane V(6,5*,6*,5), and shows approximately *D*_{2h} symmetry in the orientation related by both horizontal and vertical mirror planes V(4,8*,9*,4*,8,9) and V(6,5*,6*,5), on which the N₃[−] nitrogen atoms are located. The hydrogen atoms could not be located directly from the three-dimensional X-ray diffraction data. However, long V–O(μ) bond distances [1.894(8) and 1.930(8) Å] for V(3)–O(21) and V(7)–O(21*) bonds strongly imply hydrogen-atom co-ordination at atoms O(21) and O(21*). On the basis of bond-valence sum calculations, we find that each of these O atoms has a valence sum of 1.3–1.4 corresponding to a hydroxide (OH[−]) ligand. Such a co-ordination of two hydrogen atoms in the anion enables us to formulate the complex Na₁₂H₂[V₁₈O₄₄(N₃)]·30H₂O as Na₁₂[V₁₈O₄₂(OH)₂(N₃)]·30H₂O. The bond-valence calculations are also consistent with a charge of +5 for V(6) and V(6*). The remaining V^V in the anion is presumed to be disordered over V(1), V(2), V(5) and their symmetry equivalent (−*x*, −2 − *y*, −2 − *z*) sites, since the N...V(1) [N(1)...V(1) 3.572(2) and N(2)...V(1) 3.14(1) Å] and N...V(2) [N(1)...V(2) 3.578(2) and N(2)...V(2) 3.18(1) Å] distances for the two nearly equivalent rectangle planes V(1,2*,7*,3) and V(1*,2,7,3*) are shorter than the N...V(3) [N(1)...V(3) 3.666(2) Å and N(2)...V(3) 3.25(1) Å] and N...V(7) [N(1)...V(7) 3.707(2) and N(2)...V(7) 3.27(1) Å] distances respectively, and since the distances N...V(5) [N(1)...V(5) 4.344(2) and N(2)...V(5) 3.28(1) Å] and N...V(6) [N(1)...V(6) 4.320(2) and

Table 2 Selected atomic distances (Å) and angles (°) for cluster **1**

| | | | | | | | |
|-----------------|----------|-----------------|----------|-----------------|-----------|-----------------|-----------|
| V(1)–O(1) | 1.623(8) | V(3)–O(13) | 1.943(7) | V(5)–O(16) | 1.988(7) | V(7)–O(22) | 1.981(7) |
| V(1)–O(14) | 1.947(7) | V(3)–O(14) | 1.917(7) | V(5)–O(22) | 1.896(7) | V(8)–O(8) | 1.613(8) |
| V(1)–O(17) | 1.974(7) | V(3)–O(21) | 1.894(8) | V(6)–O(6) | 1.630(8) | V(8)–O(13) | 1.946(7) |
| V(1)–O(18) | 1.918(7) | V(4)–O(4) | 1.622(7) | V(6)–O(10) | 1.877(7) | V(8)–O(15) | 1.948(7) |
| V(1)–O(19) | 1.817(7) | V(4)–O(17) | 1.950(7) | V(6)–O(11) | 1.798(7) | V(8)–O(18) | 1.973(7) |
| V(2)–O(2) | 1.625(8) | V(4)–O(18) | 1.975(7) | V(6)–O(14) | 1.973(7) | V(8)–O(20) | 1.951(7) |
| V(2)–O(12) | 1.976(7) | V(4)–O(20) | 1.952(7) | V(6)–O(17) | 1.922(7) | V(9)–O(6) | 1.619(8) |
| V(2)–O(15) | 1.917(7) | V(4)–O(22) | 1.976(7) | V(7)–O(7) | 1.608(8) | V(9)–O(10) | 1.976(7) |
| V(2)–O(16) | 1.912(7) | V(5)–O(5) | 1.629(8) | V(7)–O(16) | 1.987(7) | V(9)–O(12) | 1.945(7) |
| V(2)–O(19) | 1.846(8) | V(5)–O(11) | 1.847(7) | V(7)–O(20) | 1.935(7) | V(9)–O(13) | 1.940(7) |
| V(3)–O(3) | 1.614(8) | V(5)–O(12) | 1.904(7) | V(7)–O(21) | 1.930(8) | V(9)–O(15) | 1.928(7) |
| V(3)–O(10) | 1.966(7) | | | | | | |
| V(1)···V(6) | 3.022(3) | V(8)···V(9) | 2.879(3) | V(5)···V(6) | 3.323(4) | V(1)···V(7) | 5.130(4) |
| V(3)···V(6) | 3.001(3) | V(1)···V(3) | 3.639(3) | V(5)···V(4*) | 3.614(3) | V(2)···V(3) | 5.156(4) |
| V(2)···V(5) | 2.974(3) | V(1)···V(2*) | 3.538(3) | V(5)···V(9) | 3.637(3) | V(4)···V(9) | 5.965(3) |
| V(4)···V(8*) | 2.964(2) | V(2)···V(7) | 3.665(3) | V(6)···V(4) | 3.609(3) | V(5)···V(6*) | 8.001(4) |
| V(5)···V(7) | 3.008(2) | V(3)···V(7*) | 3.662(3) | V(6)···V(9) | 3.591(3) | | |
| N(1)···V(1) | 3.572(2) | N(1)···V(6) | 4.320(2) | N(2)···V(2) | 3.18(1) | N(2)···V(7) | 3.27(1) |
| N(1)···V(2) | 3.578(2) | N(1)···V(7) | 3.707(2) | N(2)···V(3) | 3.25(1) | N(2)···V(9) | 3.39(1) |
| N(1)···V(3) | 3.666(2) | N(1)···V(8) | 3.746(2) | N(2)···V(5) | 3.28(1) | N(2)···V(4) | 3.40(1) |
| N(1)···V(5) | 4.344(2) | N(2)···V(1) | 3.14(1) | N(2)···V(6) | 3.24(1) | | |
| N(1)···O(19) | 3.000(8) | N(1)···O(11) | 4.749(7) | O(19)···O(21) | 2.70(1) | O(11)···O(11*) | 9.50(1) |
| N(1)···O(21) | 3.133(8) | | | O(19)···O(21*) | 5.51(1) | O(8)···O(8*) | 10.72(1) |
| V(3)–V(1)–V(7) | 92.14(7) | V(3)–V(2)–V(7) | 91.43(7) | V(9)–V(4)–V(8*) | 104.10(7) | V(2)–V(7)–V(3*) | 88.00(6) |
| V(3)–V(1)–V(2*) | 90.33(7) | V(1)–V(3)–V(7*) | 90.06(6) | V(6)–V(5)–V(6*) | 89.55(5) | V(9)–V(8)–V(4*) | 149.7(1) |
| V(7)–V(2)–V(1*) | 91.61(6) | V(1)–V(3)–V(2) | 88.14(2) | V(5)–V(6)–V(5*) | 90.45(5) | V(4)–V(9)–V(8) | 106.23(6) |

**Fig. 2** Schematic representation of the structure of $[\text{V}_{18}\text{O}_{44}(\text{N}_3)]^{14-}$ with atom labelling. Asterisked atoms are related to corresponding unasterisked ones by an inversion centre

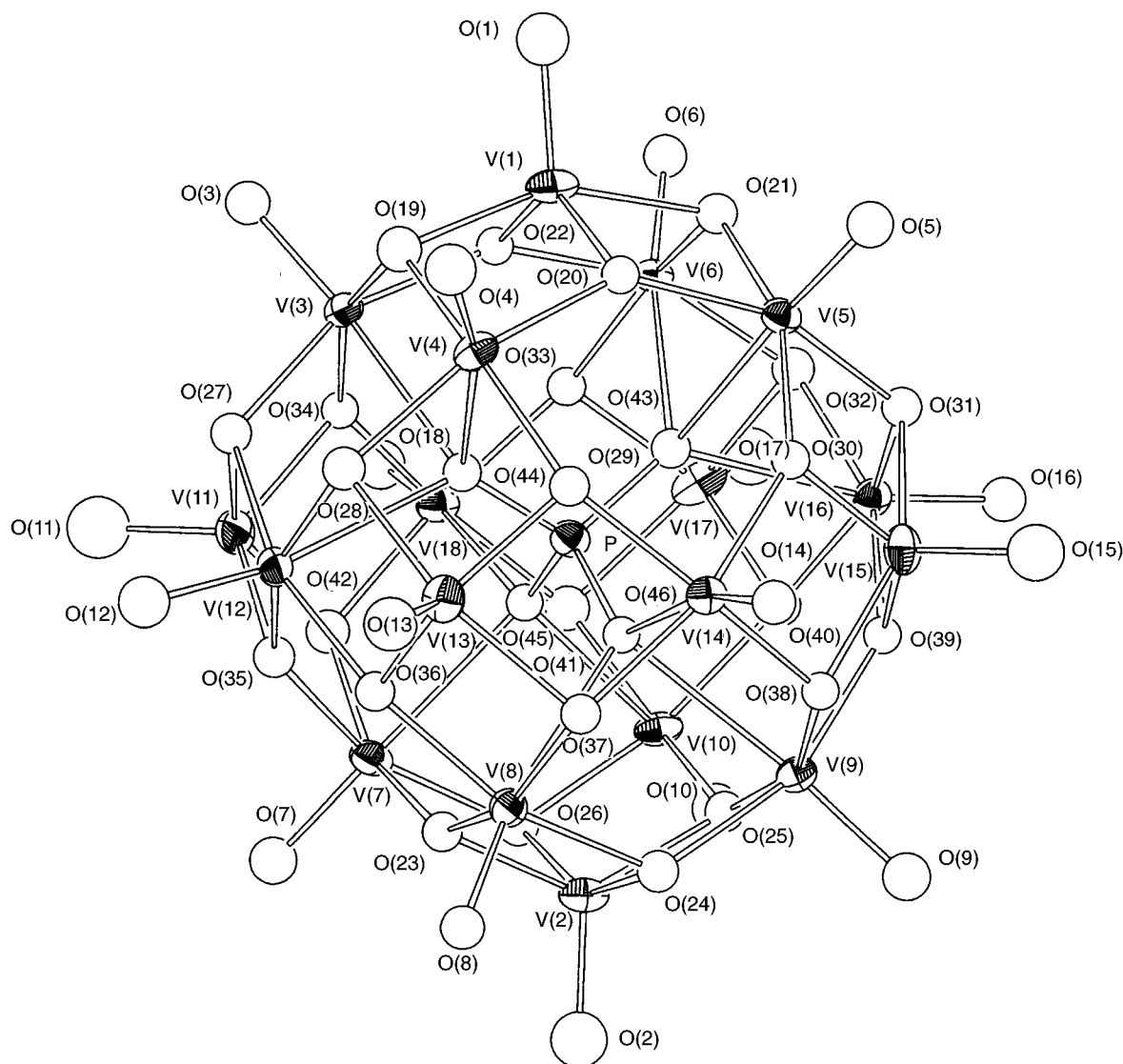


Fig. 3 Schematic representation of the structure of $[V_{18}O_{42}(PO_4)]^{11-}$ with atom labelling

$N(2) \cdots V(6)$ 3.24(1) Å] for the rectangle $V(6,5^*,6^*,5)$ plane are similar. The central nitrogen atom $N(1)$ is at distances of 3.000(8), 3.133(8) and 4.749(7) Å from three μ -oxygen atoms $O(19)$, $O(21)$ and $O(11)$, respectively. The asymmetry between the $N(1) \cdots O(19)$ and $N(1) \cdots O(21)$ distances is associated with the hydrogen-atom co-ordination on the $O(21)$ atom. Although the same anion structure has been reported for $[NEt_4]_5[H_2V_{18}O_{44}(N_3)]$ prepared by the reaction of $[NH_4]_8[H_9V_{19}O_{50}] \cdot 11H_2O$, NaN_3 and NEt_4BF_4 in water for 16 h at 75 °C, the number of vanadium(IV) centres in the anion is different from that (eight) of $[NEt_4]_5[H_2V_{18}O_{44}(N_3)]$. Such a difference of the number of the vanadium(IV) centres in the anion arises from the mechanistic difference between the photoredox self-organization of $[V_4O_{12}]^{4-}$ and the thermal decomposition of $[H_9V_{12}^{IV}V_7^{V}O_{50}]^{8-}$ to $[H_2V_{18}^{IV}V_{10}^{V}O_{44}(N_3)]^{5-}$. This may be reflected by a slight difference in the size of the cluster shell; $O(19) \cdots O(21^*)$ [5.51(1) Å] and $O(11) \cdots O(11^*)$ [9.50(1) Å] distances for **1** indicate that the $[V_{15}^{IV}V_3^{V}O_{42}(OH)_2(N_3)]^{12-}$ anion is slightly more ellipsoidal than the $[H_2V_{18}^{IV}V_{10}^{V}O_{44}(N_3)]^{5-}$ anion, since the corresponding distances for the latter were 5.60 and 9.40 Å, respectively.⁵

(b) $[V_{14}^{IV}V_4^{V}O_{42}(PO_4)]^{11-}$. The $[V_{14}^{IV}V_4^{V}O_{42}(PO_4)]^{11-}$ anion in compound **2** has the structure (superkeggin structure) of an α -Keggin core with six additional five-co-ordinate terminal VO units capping the pits on every side of the Keggin unit that lie on three C_2 axes. This superkeggin structure was observed for

$[V_{18}^{IV}O_{42}(VO_4)]^{15-}$ and $[V_{12}^{IV}V_6^{V}O_{42}(SO_4)]^{8-}$.⁶ The structure is disorder-free and can be regarded as the same as that of the 1:14 vanadophosphate $[PV_{14}^{IV}O_{42}]^{9-}$ with four additional square-pyramidal {VO} units.^{20,21} Another polyoxovanadophosphate containing an α -Keggin core with a central PO_4 unit has been prepared using a hydrothermal technique; a reduced complex $[P^{IV}Mo^V_6O_{40}(V^{IV}O)_2]^{5-}$ is capped on opposite Mo_4O_4 rectangles by $V^{IV}O$.²² Table 3 shows selected bond distances and angles. The $V=O$, $V-O(\mu_3)$ and $V-O(\mu_4)$ bond distances are 1.59(1)–1.64(1), 1.86(1)–2.02(1) and 2.41(1)–2.53(1) Å, respectively, indicating the expected trend of increasing V–O bond length for one- < three- < four-co-ordinate oxygens. The central PO_4 tetrahedral environment involves O–P–O angles ranging from 108.8(7) to 110.3(7)° and a mean P–O bond distance of 1.54(1) Å. Fig. 6 shows the co-ordination geometries at the capping five-co-ordinate OVO_4 square pyramidal and the Keggin six-co-ordinate VO_6 octahedral centres. Each of the six capping vanadium centres adopts a distorted trigonal-bipyramidal co-ordination geometry. Three kinds of neighbouring $V \cdots V$ distances are observed; 2.833(5)–2.985(5) Å [mean 2.904(1) Å] between V atoms of the edge-sharing OVO_4 square pyramid and VO_6 octahedron, 3.409(4)–3.500(5) Å [mean 3.470(1) Å] for the edge-sharing VO_6 octahedra in the α -Keggin core, and 3.693(4)–3.740(5) Å [mean 3.721(1) Å] for the corner-sharing VO_6 octahedra in the α -Keggin core. Comparison of the neighbouring $V \cdots V$ distances between **1** and **2** reveals increasing mean $V \cdots V$ distance for the edge-

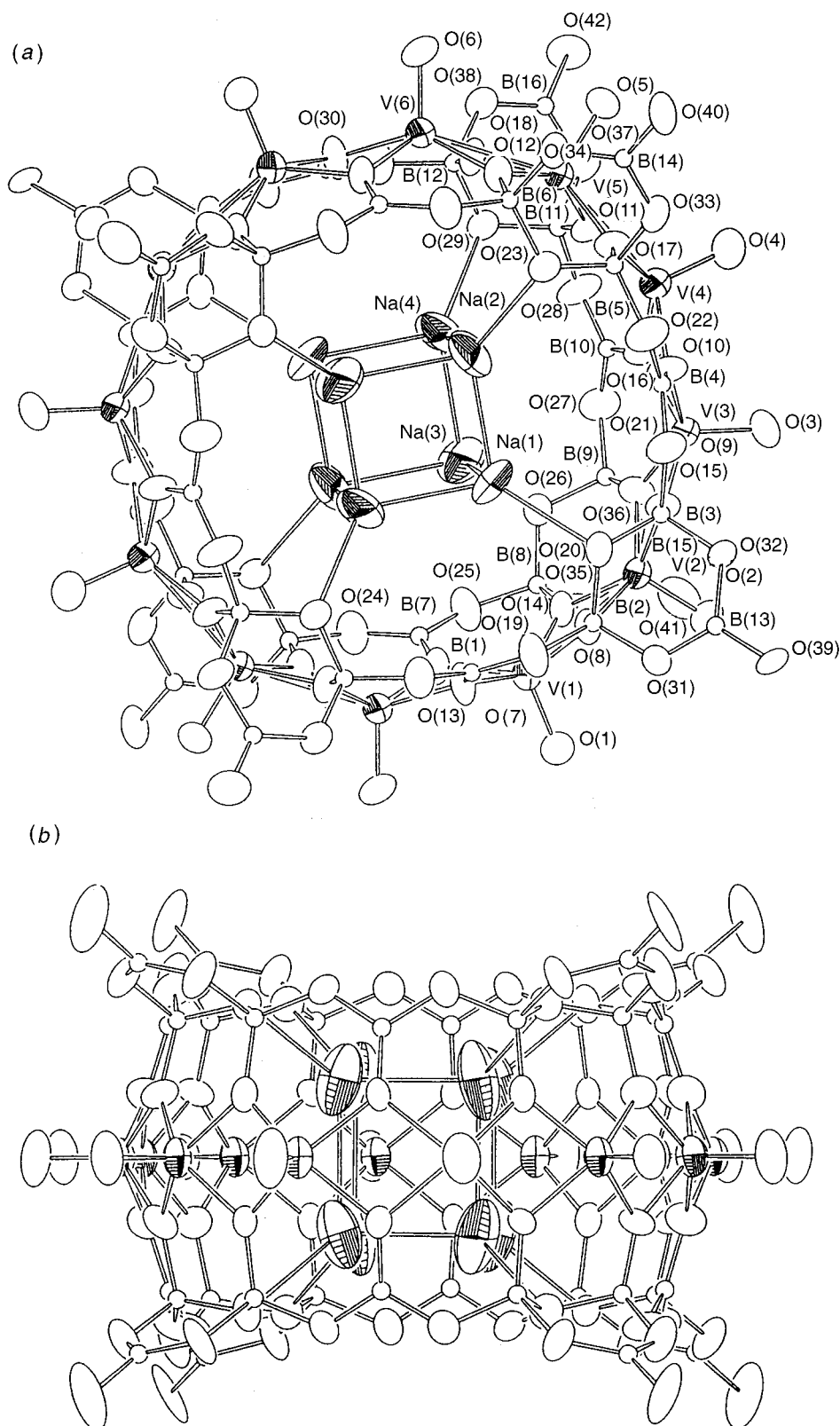


Fig. 4 Schematic representations of the structure of $[V_{12}B_{32}O_{84}Na_4]^{19-}$ with atom labelling: (a) and (b) indicate the ring cross-section and a side view of the area of least curvature, respectively. Asterisked atoms are related to corresponding unasterisked ones by an inversion centre. Each sodium atom has half occupancy

sharing OVO_4 or OVO_4/VO_6 (2.8–3.0) < edge-sharing VO_6 (3.4–3.5) < corner-sharing OVO_4 (3.3–3.7) < corner-sharing VO_6 (3.7–3.8 Å) polyhedra. The $V \cdots V$ distances between *trans* capping V atoms are 7.862(4)–7.901(4) [mean 7.883(2) Å]. These distances are longer than the $V \cdots V$ 7.157(5)–7.241(4) Å [mean 7.191(2) Å] for the α -Keggin core diameter. The difference (0.7 Å) between the two distances indicates the distortion from a perfect spherical cluster shell. The P–O bonding of four

sets [V(5,6,16), V(3,4,12), V(7,10,18) and V(8,9,14)] of edge-shared V_3O_{13} units through the $O(\mu_4)$ atoms O(43), O(44), O(45) and O(46) leads to a change from a square to a rectangle for each pit.

(c) $[V^{IV}_7V^V_5B_{32}O_{84}]^{19-}$. The $[V^{IV}_7V^V_5B_{32}O_{84}]^{19-}$ anion in compound **3** consists of a cyclic belt-shaped $(VO)_{12}O_{24}$ array of edge-sharing OVO_4 square pyramids, doubly bridged by BO_3

Table 3 Selected atomic distances (Å) and angles (°) for cluster **2**

| | | | | | | | |
|------------------|----------|------------------|----------|------------------|----------|------------------|----------|
| V(1)–O(1) | 1.63(1) | V(5)–O(20) | 1.98(1) | V(10)–O(10) | 1.62(1) | V(14)–O(30) | 1.94(1) |
| V(1)–O(22) | 1.86(1) | V(5)–O(43) | 2.50(1) | V(10)–O(40) | 1.92(1) | V(14)–O(29) | 1.96(1) |
| V(1)–O(19) | 1.98(1) | V(6)–O(6) | 1.63(1) | V(10)–O(26) | 1.94(1) | V(14)–O(46) | 2.48(1) |
| V(1)–O(20) | 1.89(1) | V(6)–O(32) | 1.93(1) | V(10)–O(41) | 1.95(1) | V(15)–O(15) | 1.61(1) |
| V(1)–O(21) | 1.99(1) | V(6)–O(21) | 1.95(1) | V(10)–O(25) | 1.97(1) | V(15)–O(30) | 1.86(1) |
| V(2)–O(2) | 1.61(1) | V(6)–O(22) | 1.95(1) | V(10)–O(45) | 2.53(1) | V(15)–O(39) | 1.90(1) |
| V(2)–O(23) | 1.87(1) | V(6)–O(33) | 1.96(1) | V(11)–O(11) | 1.60(2) | V(15)–O(38) | 1.97(1) |
| V(2)–O(25) | 1.90(1) | V(6)–O(43) | 2.43(1) | V(11)–O(34) | 1.87(1) | V(15)–O(31) | 1.98(1) |
| V(2)–O(24) | 1.97(1) | V(7)–O(7) | 1.61(1) | V(11)–O(35) | 1.86(1) | V(16)–O(16) | 1.59(1) |
| V(2)–O(26) | 1.98(1) | V(7)–O(23) | 1.95(1) | V(11)–O(27) | 1.97(1) | V(16)–O(31) | 1.95(1) |
| V(3)–O(3) | 1.62(1) | V(7)–O(42) | 1.95(1) | V(11)–O(42) | 1.99(1) | V(16)–O(32) | 1.93(1) |
| V(3)–O(22) | 1.92(1) | V(7)–O(26) | 1.96(1) | V(12)–O(12) | 1.60(1) | V(16)–O(39) | 1.95(1) |
| V(3)–O(27) | 1.94(1) | V(7)–O(35) | 1.96(1) | V(12)–O(36) | 1.93(1) | V(16)–O(40) | 1.95(1) |
| V(3)–O(19) | 1.96(1) | V(7)–O(45) | 1.41(1) | V(12)–O(27) | 1.97(1) | V(16)–O(43) | 2.51(1) |
| V(3)–O(34) | 1.96(1) | V(8)–O(8) | 1.62(1) | V(12)–O(28) | 1.95(1) | V(17)–O(17) | 1.64(2) |
| V(3)–O(44) | 2.44(1) | V(8)–O(23) | 1.93(1) | V(12)–O(35) | 1.96(1) | V(17)–O(33) | 1.88(1) |
| V(4)–O(4) | 1.63(2) | V(8)–O(24) | 1.94(1) | V(12)–O(44) | 2.45(1) | V(17)–O(40) | 1.91(1) |
| V(4)–O(20) | 1.94(1) | V(8)–O(37) | 1.96(1) | V(13)–O(13) | 1.63(2) | V(17)–O(32) | 2.01(1) |
| V(4)–O(28) | 1.95(1) | V(8)–O(36) | 1.97(1) | V(13)–O(36) | 1.87(1) | V(17)–O(41) | 2.02(1) |
| V(4)–O(29) | 1.95(1) | V(8)–O(46) | 2.50(1) | V(13)–O(29) | 1.87(1) | V(18)–O(18) | 1.60(2) |
| V(4)–O(19) | 1.98(1) | V(9)–O(9) | 1.64(1) | V(13)–O(28) | 1.96(1) | V(18)–O(41) | 1.92(1) |
| V(4)–O(44) | 2.50(1) | V(9)–O(39) | 1.94(1) | V(13)–O(37) | 1.98(1) | V(18)–O(42) | 1.92(1) |
| V(5)–O(5) | 1.61(1) | V(9)–O(25) | 1.95(1) | V(14)–O(14) | 1.63(1) | V(18)–O(33) | 1.93(1) |
| V(5)–O(30) | 1.94(1) | V(9)–O(38) | 1.95(1) | V(14)–O(37) | 1.91(1) | V(18)–O(34) | 1.94(1) |
| V(5)–O(21) | 1.96(1) | V(9)–O(24) | 1.97(1) | V(14)–O(38) | 1.91(1) | V(16)–O(45) | 2.42(1) |
| V(5)–O(31) | 1.96(1) | | | | | | |
| P–O(43) | 1.53(1) | P–O(46) | 1.54(1) | O(43)–P–O(46) | 109.1(7) | O(46)–P–O(45) | 109.0(7) |
| P–O(44) | 1.54(1) | P–O(45) | 1.56(1) | O(46)–P–O(44) | 110.3(7) | O(43)–P–O(45) | 109.5(7) |
| | | | | O(43)–P–O(44) | 110.1(7) | O(44)–P–O(45) | 108.8(7) |
| V(1)···V(2) | 7.901(4) | V(13)···V(17) | 7.885(4) | V(3)···V(4) | 3.491(5) | V(2)···V(9) | 2.908(4) |
| V(3)···V(9) | 7.196(4) | V(14)···V(18) | 7.167(4) | V(3)···V(6) | 3.725(4) | V(2)···V(10) | 2.985(5) |
| V(4)···V(10) | 7.241(4) | V(1)···V(3) | 2.845(5) | V(4)···V(5) | 3.693(4) | V(7)···V(8) | 3.731(5) |
| V(5)···V(7) | 7.169(4) | V(1)···V(4) | 2.950(5) | V(5)···V(6) | 3.460(4) | V(7)···V(10) | 3.461(5) |
| V(6)···V(8) | 7.157(5) | V(1)···V(5) | 2.973(5) | V(2)···V(7) | 2.897(4) | V(8)···V(9) | 3.490(4) |
| V(11)···V(15) | 7.862(4) | V(1)···V(6) | 2.864(5) | V(2)···V(8) | 2.833(5) | V(9)···V(10) | 3.696(4) |
| V(12)···V(16) | 7.214(4) | | | | | | |
| O(1)–V(1)–O(22) | 113.8(6) | O(22)–V(1)–O(19) | 85.4(5) | O(3)–V(3)–O(19) | 99.5(6) | O(22)–V(3)–O(27) | 156.5(5) |
| O(1)–V(1)–O(20) | 118.7(6) | O(19)–V(1)–O(21) | 150.3(5) | O(3)–V(3)–O(34) | 101.5(6) | O(22)–V(3)–O(19) | 84.2(5) |
| O(1)–V(1)–O(19) | 105.4(6) | O(3)–V(3)–O(26) | 102.7(5) | O(3)–V(3)–O(44) | 167.4(5) | O(22)–V(3)–O(34) | 87.1(5) |
| O(1)–V(1)–O(21) | 104.2(6) | O(3)–V(3)–O(27) | 99.8(6) | O(19)–V(3)–O(34) | 158.6(5) | O(22)–V(3)–O(44) | 86.8(4) |
| O(22)–V(1)–O(20) | 127.6(5) | | | | | | |

and BO_4 groups to produce a doughnut-shaped structure with approximately D_{4h} symmetry, as shown in Fig. 4. To our knowledge there are no examples known of polyboratovanadates with a cyclic dodecagonal array of OVO_4 square pyramids, although the cyclic belt-shaped octanuclear polyoxo-alkoxovanadate(IV) $[\text{V}_8\text{O}_8(\text{OMe})_{16}]$ was found in $[\text{NBu}_4]_2[\text{V}_8\text{O}_8(\text{OMe})_{16}(\text{C}_2\text{O}_4)]$ where it encircles an oxalate anion.²³ Interatomic distances and angles are listed in Table 4. The $(\text{VO})_{12}\text{O}_{24}$ array constitutes a cyclic tiara framework of OVO_4 square pyramids with $\text{V}=\text{O}$ and $\text{V}-\text{O}(\mu_3)$ bond distances of 1.59(1)–1.648(9) and 1.89(1)–1.99(1) Å, respectively. Each $\text{V}-\text{O}$ bridging oxygen atom is bound to B atoms at B–O bond lengths of 1.32(2)–1.53(2) Å. The resultant cyclic hexadecaborate framework sandwiches almost symmetrically the cyclic dodecavanadate framework. In the cyclic hexadecaborate each BO_4 tetrahedron of the vertex-sharing, six-membered B_3O_3 ring, which consists of two tetrahedral BO_4 and one triangular BO_3 groups, is linked by a three-co-ordinate B atom to form a $\text{B}_{16}\text{O}_{24}$ ring. Fig. 7 shows the vertex-sharing B_3O_3 ring unit. The terminal B–O bond distances of 1.37(2)–1.45(2) Å [mean 1.42(1) Å] for the BO_3 triangle in the B_3O_3 ring are longer than the bridging B–O bond distances of 1.32(2)–1.39(2) Å [mean 1.36(1) Å] for the BO_3 triangle linking two B_3O_3 rings. Each B atom of BO_3 occupies a distorted triangular planar site, while each B of BO_4 resides in a distorted tetrahedral site. Valence-sums are 0.8(1)–1.1(1) for the O(39), O(40), O(41) and O(42) atoms. By contrast, those for other oxygen atoms that carry

a formal negative charge in the anion are 1.5(1)–2.2(1). This implies the co-ordination of hydrogen atoms on the terminal BO_3 oxygen atom of the B_3O_3 ring with a resultant formula change of $[\text{V}^{\text{IV}}_7\text{V}^{\text{V}}_5\text{B}_{32}\text{O}_{84}]^{19-}$ to $[\text{V}^{\text{IV}}_7\text{V}^{\text{V}}_5\text{B}_{32}(\text{OH})_8\text{O}_{76}]^{11-}$. The short distances between the terminal BO_3 and lattice-water oxygen atoms O(39)···O(48) [2.82(3) Å], O(40)···O(49^I) [2.92(3) Å], O(41)···O(45^{II}) [2.79(2) Å] and O(42)···O(50^{III}) [2.92(3) Å], where I, II and III indicate symmetry equivalents ($1-x, -y, -1-z$), ($-x, 1-y, -1-z$) and ($-x, 1-y, -z$) respectively, suggest the involvement of a hydrogen-bonding proton between these oxygen atoms. The boron and vanadium frameworks in the anion are shown in Fig. 8 where the edge-sharing V_{12} -vanadate ring {at the neighbouring $\text{V}\cdots\text{V}$ distances of 2.893(4)–3.035(4) Å [mean 2.968(2) Å] with a mean $\text{V}\cdots\text{V}$ diameter of 11.37(2) Å} is co-ordinated by two vertex-sharing B_{12} -borate rings at the neighbouring $\text{B}\cdots\text{B}$ distances of 2.40(3)–2.61(3) Å [mean 2.50(1) Å] with a mean $\text{B}\cdots\text{B}$ diameter of 9.79(2) Å from either side. Two B_{12} least-square planes are parallel with a mean distance of 5.22(2) Å and have eight B_3 triangle horns which constitute B_3O_3 rings with dihedral angles of 148–152° (mean 150°). The large cavity produced by the cyclic $[\text{V}^{\text{IV}}_7\text{V}^{\text{V}}_5\text{B}_{32}(\text{OH})_8\text{O}_{76}]^{11-}$ unit with highly negative charges is occupied by a cationic Na_4 moiety. Each Na atom is bound to the B_3O_3 ring oxygen atom with the Na–O vector oriented in a chair-like arrangement; the $[\text{Na}(1), \text{B}(2), \text{B}(3)]$, $[\text{Na}(2), \text{B}(5), \text{B}(6)]$, $[\text{Na}(3), \text{B}(8), \text{B}(9)]$ and $[\text{Na}(4), \text{B}(11), \text{B}(12)]$ planes are approximately parallel to the $[\text{O}(39), \text{O}(31), \text{O}(32)]$,

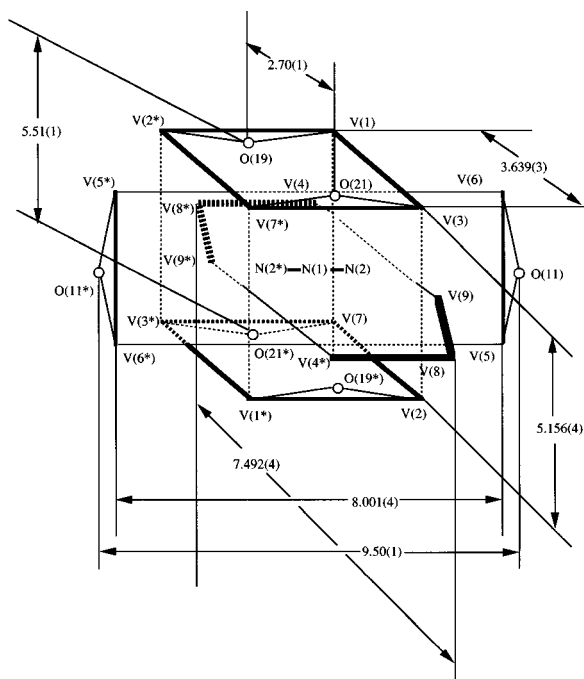


Fig. 5 Vanadium framework for the anion of cluster **1**. Thick lines imply that OVO_4 square pyramids share edges. Atoms N(1), N(2), O(11), O(19), O(21) and their symmetry equivalents are included for clarification. Asterisked atoms are related to corresponding unasterisked ones by an inversion centre. Distances are in Å

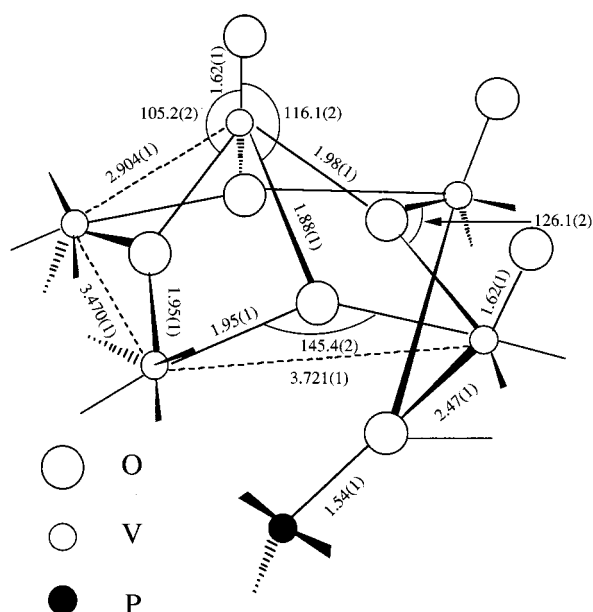


Fig. 6 Co-ordination geometry of the terminal VO unit capping the pit of the Keggin unit for cluster **2**. Distances (Å) and angles (°) are mean values

[O(40),O(33),O(34)], [O(41),O(35),O(36)] and [O(42),O(37),O(38)] planes, respectively (with dihedral angles 169–172°), and make a dihedral angle of about 20 (20–23°) with the B₁₂ least-squares plane.

Magnetic measurements

Temperature dependences of the product χT for compounds **1**–**3** are shown in Fig. 9 where χ is the molar magnetic susceptibility and T the temperature. The downturns seen in the data reveal antiferromagnetic couplings in the three complexes.²⁴ For **1** initially χT decreases slightly on decreasing temperature, and it stabilizes at about $\chi T = 3.64$ emu mol^{−1} K (effective magnetic moment $\mu_{\text{eff}} = 5.40 \mu_{\text{B}}$) in the range 250–50 K. Below 50 K χT

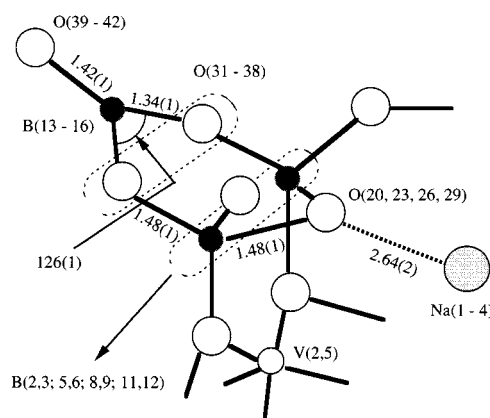


Fig. 7 Co-ordination environment of the vertex-sharing B₃O₃ ring unit in cluster **3**. Distances (Å) and angles (°) are mean values

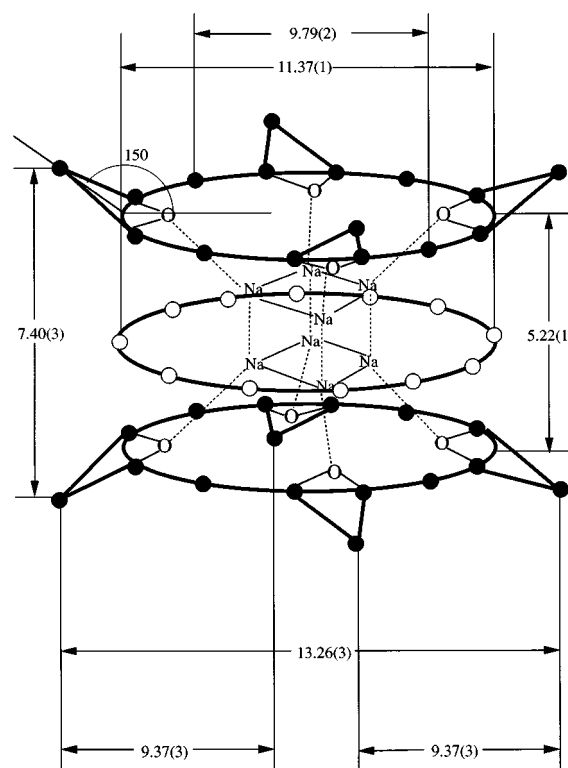


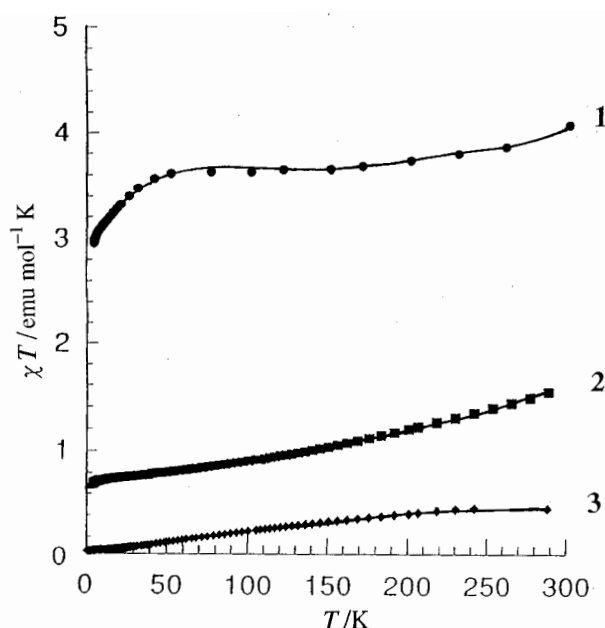
Fig. 8 Boron (●) and vanadium (○) frameworks of the anion in cluster **3**. Distances (Å) and angles (°) are mean values

decreases rapidly reaching 2.9 emu mol⁻¹ K at 4.2 K. For **2** and **3**, on the other hand, the temperature dependence of χT indicates that the room-temperature values [1.55 emu mol⁻¹ K ($\mu_{\text{eff}} = 3.52 \mu_{\text{B}}$) for **2** and 0.44 emu mol⁻¹ K ($\mu_{\text{eff}} = 1.88 \mu_{\text{B}}$) for **3** corresponding to four ($\mu_{\text{eff}} = 3.46 \mu_{\text{B}}$) and one ($\mu_{\text{eff}} = 1.73 \mu_{\text{B}}$) uncoupled electrons, respectively] are much smaller than for **1** [4.03 emu mol⁻¹ K ($\mu_{\text{eff}} = 5.68 \mu_{\text{B}}$) corresponding to the value expected for eleven uncoupled electrons ($\mu_{\text{eff}} = 5.74 \mu_{\text{B}}$)] and that the χT product decreases with decreasing temperature at $T > 50$ K without a plateau.

Since the antiferromagnetic exchange interaction can be explained by the distribution of the short $\text{V}^{\text{IV}} \cdots \text{V}^{\text{IV}}$ distances which determines the spin polarization,²⁵ in compound **1** the shortest distance [2.879(3) Å] of $\text{V}(8) \cdots \text{V}(9)$ and $\text{V}(8^*) \cdots \text{V}(9^*)$ lies in the range expected for antiferromagnetic coupling, to leave the eleven vanadium(IV) centres ($S=12$) largely uncoupled in the $[\text{V}_{15}^{\text{IV}}\text{V}_3^{\text{V}}\text{O}_{44}(\text{N}_3)]^{14-}$ anion. In the low-temperature range weak coupling occurs in either $\text{V}(2) \cdots \text{V}(5)$ or $\text{V}(2^*) \cdots \text{V}(5^*)$ [2.974(3) Å], leaving nine vanadium(IV) centres ($S=10$) uncoupled in the anion. We interpret the temperature dependence of χT at $T > 50$ K as indicating a mixture

Table 4 Selected atomic distances (Å) and angles (°) for cluster **3**

| | | | | | | | |
|------------------------------|----------|----------------|----------|-----------------------------|----------|-------------------------------|----------|
| V(1)–O(1) | 1.60(1) | V(2)–O(14) | 1.919(9) | V(4)–O(10) | 1.95(1) | V(5)–O(17) | 1.952(9) |
| V(1)–O(7) | 1.96(1) | V(2)–O(15) | 1.92(1) | V(4)–O(11) | 1.934(9) | V(5)–O(18) | 1.94(1) |
| V(1)–O(8) | 1.89(1) | V(3)–O(3) | 1.601(9) | V(4)–O(16) | 1.96(1) | V(6)–O(6) | 1.62(1) |
| V(1)–O(13) | 1.981(9) | V(3)–O(9) | 1.90(1) | V(4)–O(17) | 1.91(1) | V(6)–O(7) | 1.986(9) |
| V(1)–O(14) | 1.89(1) | V(3)–O(10) | 1.958(9) | V(5)–O(5) | 1.635(9) | V(6)–O(12) | 1.91(1) |
| V(2)–O(2) | 1.648(9) | V(3)–O(15) | 1.93(1) | V(5)–O(11) | 1.93(1) | V(6)–O(13) | 1.99(1) |
| V(2)–O(8) | 1.92(1) | V(3)–O(16) | 1.97(1) | V(5)–O(12) | 1.950(9) | V(6)–O(18) | 1.90(1) |
| V(2)–O(9) | 1.944(9) | V(4)–O(4) | 1.59(1) | | | | |
| B(1)–O(7) | 1.32(2) | B(5)–O(11) | 1.51(2) | B(8)–O(35) | 1.49(2) | B(12)–O(30) | 1.50(2) |
| B(1)–O(19) | 1.39(2) | B(5)–O(22) | 1.53(2) | B(9)–O(15) | 1.48(2) | B(12)–O(38) | 1.48(2) |
| B(1)–O(30) | 1.37(2) | B(5)–O(23) | 1.47(2) | B(9)–O(26) | 1.47(2) | B(12)–O(31) | 1.32(2) |
| B(2)–O(8) | 1.51(2) | B(5)–O(33) | 1.51(2) | B(9)–O(27) | 1.49(2) | B(13)–O(32) | 1.35(2) |
| B(2)–O(19) | 1.50(2) | B(6)–O(12) | 1.41(2) | B(9)–O(36) | 1.45(2) | B(13)–O(39) | 1.45(2) |
| B(2)–O(20) | 1.47(2) | B(6)–O(23) | 1.47(2) | B(10)–O(16) | 1.36(2) | B(14)–O(33) | 1.34(2) |
| B(2)–O(31) | 1.50(2) | B(6)–O(24) | 1.52(2) | B(10)–O(27) | 1.38(2) | B(14)–O(34) | 1.35(2) |
| B(3)–O(9) | 1.46(2) | B(6)–O(34) | 1.52(2) | B(10)–O(28) | 1.36(2) | B(14)–O(40) | 1.41(2) |
| B(3)–O(20) | 1.45(2) | B(7)–O(13) | 1.34(2) | B(11)–O(17) | 1.50(2) | B(15)–O(35) | 1.31(2) |
| B(3)–O(21) | 1.52(2) | B(7)–O(24) | 1.36(2) | B(11)–O(28) | 1.49(2) | B(15)–O(36) | 1.37(2) |
| B(3)–O(32) | 1.48(2) | B(7)–O(25) | 1.36(2) | B(11)–O(29) | 1.45(2) | B(15)–O(41) | 1.45(2) |
| B(4)–O(10) | 1.36(2) | B(8)–O(14) | 1.51(2) | B(11)–O(37) | 1.46(2) | B(16)–O(37) | 1.35(2) |
| B(4)–O(21) | 1.36(2) | B(8)–O(25) | 1.51(2) | B(12)–O(18) | 1.44(2) | B(16)–O(38) | 1.36(2) |
| B(4)–O(22) | 1.38(2) | B(8)–O(26) | 1.43(2) | B(12)–O(29) | 1.50(2) | B(16)–O(42) | 1.37(2) |
| V(1)···V(2) | 2.893(4) | V(4)···V(5) | 2.906(4) | V(1)···V(1*) | 11.37(1) | V(1)–V(2)–V(3) | 149.6(1) |
| V(2)···V(3) | 2.903(4) | V(5)···V(6) | 2.900(4) | V(3)···V(3*) | 11.35(1) | | |
| V(3)···V(4) | 3.027(4) | V(6)···V(1*) | 3.035(4) | | | | |
| O(45)···O(41 ^{II}) | 2.79(2) | O(48)···O(39) | 2.82(3) | O(49)···O(40 ^I) | 2.92(3) | O(50)···O(42 ^{III}) | 2.92(3) |
| Na(1)–O(20) | 2.62(2) | Na(1)···Na(2) | 2.62(2) | Na(1)···Na(2*) | 3.99(2) | Na(2)–Na(1)–Na(3) | 89.3(6) |
| Na(2)–O(23) | 2.64(2) | Na(1)···Na(3) | 2.96(3) | Na(2)···Na(4*) | 3.69(2) | Na(1)–Na(2)–Na(4) | 90.0(8) |
| Na(3)–O(26) | 2.65(2) | Na(2)···Na(4) | 2.99(3) | Na(3)···Na(2) | 3.94(2) | | |
| Na(4)–O(29) | 2.63(2) | Na(3)···Na(4) | 2.61(2) | | | | |
| B(1)···B(2) | 2.60(3) | B(5)···B(14) | 2.47(3) | B(9)···B(15) | 2.43(3) | B(2)···B(8) | 5.38(4) |
| B(2)···B(3) | 2.45(3) | B(6)···B(14) | 2.46(2) | B(10)···B(11) | 2.57(3) | B(4)···B(10) | 5.01(3) |
| B(2)···B(13) | 2.40(3) | B(6)···B(7*) | 2.57(3) | B(11)···B(12) | 2.48(3) | B(13)···B(15) | 7.40(3) |
| B(3)···B(4) | 2.59(3) | B(7)···B(8) | 2.59(3) | B(11)···B(16) | 2.44(3) | B(14)···B(16) | 7.50(3) |
| B(3)···B(13) | 2.42(3) | B(8)···B(9) | 2.43(3) | B(12)···B(16) | 2.47(3) | B(1)···B(7*) | 9.49(3) |
| B(4)···B(5) | 2.60(3) | B(8)···B(15) | 2.40(3) | B(1)···B(7) | 4.98(3) | B(4)···B(10*) | 9.51(3) |
| B(5)···B(6) | 2.46(3) | B(9)···B(10) | 2.61(3) | | | | |
| B(1)–B(2)–B(3) | 145(1) | B(3)–B(4)–B(5) | 157(1) | B(6)–B(5)–B(14) | 59.8(8) | | |

Symmetry codes: * $-x, -y, -z$; I $1-x, -y, -1-z$; II $-x, 1-y, -1-z$; III $-x, 1-y, -z$.**Fig. 9** Temperature dependences of χT for clusters **1–3**

of two spin states $S = 12$ and 10 . Thus, the intermediate spin state $S = 11$ ($3.75 \text{ emu mol}^{-1} \text{ K}$, $5.48 \mu_B$) is formally observed at

the plateau (Fig. 9). A similar interpretation has been made for the spin states of $[\text{V}_{18}\text{O}_{42}\text{Cl}]^{13-}$ and $[\text{V}_{18}\text{O}_{42}(\text{H}_2\text{O})]^{12-}$.² Fig. 10 shows exchange pathways in $[\text{V}^{\text{IV}}_{15}\text{V}^{\text{V}}_3\text{O}_{44}(\text{N}_3)]^{14-}$ for $S = 12$ and 10 where $\text{V}(2^*)$ is assumed to be in the $+5$ oxidation state, in addition to $\text{V}(6)$ and $\text{V}(6^*)$. The low-spin states $S = 5$ for **2** and $S = 2$ for **3** at room temperature are associated with either delocalization or disordering of the vanadium(IV) centres. It is reasonable to assume that in **2** the hopping of the d^1 electron at the $\text{V}^{\text{IV}}\text{O}_6$ octahedron in the α -Keggin core occurs over the corner-sharing VO_6 octahedra with a $\text{V}–\text{O}–\text{V}$ bond angle of about 150° [$140.6(7)–149.8(7)^\circ$].²⁶ This allows us to consider the antiferromagnetic exchange interaction between capped and α -Keggin-core vanadium(IV) centres, because of the short distances [mean $2.904(1) \text{ Å}$] between the capped- and Keggin-core V atoms. Therefore, uncoupled vanadium(IV) centres in **2** will be identified as the capped sites, although the mixed valency of **2** adds uncertainties as to the relative location of paramagnetic centres. In **3** the short neighbouring $\text{V} \cdots \text{V}$ distances $\text{V}(1) \cdots \text{V}(2)$ [$2.893(4) \text{ Å}$], $\text{V}(2) \cdots \text{V}(3)$ [$2.903(4) \text{ Å}$], $\text{V}(4) \cdots \text{V}(5)$ [$2.906(4) \text{ Å}$] and $\text{V}(5) \cdots \text{V}(6)$ [$2.900(4) \text{ Å}$] for the cyclic $(\text{VO})_{12}\text{O}_{24}$ array indicate the disorder of seven vanadium(IV) centres among the edge-sharing OVO_4 square pyramids, leading to a strong antiferromagnetic coupling between the vanadium(IV) sites. Therefore, it is reasonable to consider that the occurrence of three sets of the antiferromagnetic couplings on the $[\text{V}^{\text{IV}}_7\text{V}^{\text{V}}_5\text{B}_{32}\text{O}_{84}]^{19-}$ anion leaves

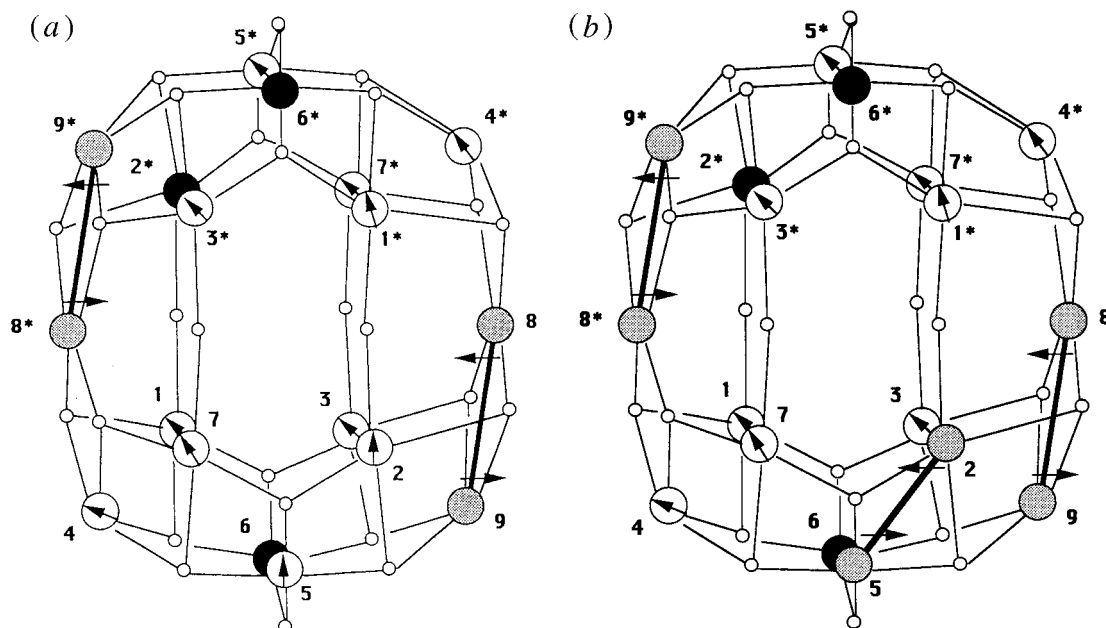


Fig. 10 Schematic spin arrangement preferred for eleven uncoupled [(a) at room temperature] and nine uncoupled [(b) at low temperature] $S = \frac{1}{2}$ spins in cluster 1. Numbers and stick lines denote the vanadium atoms and spin pairing in $V^{IV} \cdots V^{IV}$ pairs. Filled circles indicate vanadium(V) centres which are assumed to be V(6), V(6*) and V(2*)

one vanadium(IV) centre ($S = 2$ state) uncoupled in the anion. If only a weak antiferromagnetic coupling is considered for the decreasing spin state at low temperature, only the inter-molecular coupling between the d_{xy} magnetic orbitals of the V^{IV} would contribute in **3** where the nearest $V \cdots V$ distance between two anions is 9.582(5) Å. Both delocalization and disorder of vanadium(IV) centres in **2** and **3** elucidate the regular downturns for χT with decreasing temperature. At low temperature, as far as the magnetic behaviour is concerned, weak intra- and inter-molecular exchange interactions play some role.

Acknowledgements

We acknowledge a Grant-in-Aid for Scientific Research, No. 06403011, from the Ministry of Education, Science, Sports and Culture for support of this work.

References

- 1 Part 1, T. Yamase and K. Ohtaka, *J. Chem. Soc., Dalton Trans.*, 1994, 2599.
- 2 Part 2, T. Yamase, K. Ohtaka and M. Suzuki, *J. Chem. Soc., Dalton Trans.*, 1996, 283.
- 3 M. T. Pope and A. Müller, *Angew. Chem., Int. Ed. Engl.*, 1991, **30**, 34 and refs. therein.
- 4 A. Müller, H. Reuter and S. Dillinger, *Angew. Chem., Int. Ed. Engl.*, 1995, **34**, 2328.
- 5 A. Müller, E. Krickemeyer, M. Penk, R. Rohlfing, A. Armatage and H. Bögge, *Angew. Chem., Int. Ed. Engl.*, 1991, **30**, 1674.
- 6 A. Müller, J. Döring, H. Bögge and E. Krickemeyer, *Chimia*, 1988, **42**, 300.
- 7 J. Fischer, L. Ricard and R. Weiss, *J. Am. Chem. Soc.*, 1976, **98**, 3050; M. Michelon, G. Hervé and M. Leyrie, *J. Inorg. Nucl. Chem.*, 1980, **42**, 1583.
- 8 M. Leyrie and G. Hervé, *Nouv. J. Chim.*, 1978, **2**, 233; F. Robert, M. Leyrie, G. Hervé, A. Tézé and Y. Jeannin, *Inorg. Chem.*, 1980, **19**, 1746.
- 9 T. L. Jorjris, M. Kozik and L. C. Baker, *Inorg. Chem.*, 1990, **29**, 1746.
- 10 M. H. Alizadeh, S. P. Harmalker, Y. Jeannin, J. Martin-Frère and M. T. Pope, *J. Am. Chem. Soc.*, 1985, **107**, 2662.
- 11 P. Román, A. San José, A. Luque and J. M. Gutiérrez-Zorrilla, *Inorg. Chem.*, 1993, **32**, 775.
- 12 C. J. O'Connor, *Prog. Inorg. Chem.*, 1982, **29**, 203.
- 13 G. M. Sheldrick, *Crystallographic Computing 3*, eds. G. M. Sheldrick, C. Kruger and R. Goddard, Oxford University Press, 1985, p. 175.
- 14 G. J. Gilmore, *J. Appl. Crystallogr.*, 1984, **42**, 46.
- 15 A. C. T. North, D. C. Phillips and F. S. Mathews, *Acta Crystallogr., Sect. A*, 1968, **24**, 351.
- 16 N. Walker and D. Stuart, *Acta Crystallogr., Sect. A*, 1983, **158**, 3.
- 17 TEXSAN, Single-crystal Structure Analysis Software, Molecular Structure Corporation, The Woodlands, TX, 1989.
- 18 I. D. Brown and K. K. Wu, *Acta Crystallogr., Sect. B*, 1976, **32**, 1957.
- 19 D. Altermatt and I. D. Brown, *Acta Crystallogr., Sect. B*, 1985, **41**, 240; I. D. Brown and D. Altermatt, *Acta Crystallogr., Sect. B*, 1985, **41**, 144.
- 20 R. Kato, A. Kobayashi and Y. Sasaki, *J. Am. Chem. Soc.*, 1980, **102**, 6572.
- 21 M. J. Khan, J. Zubietta and P. Toscano, *Inorg. Chim. Acta*, 1992, **193**, 17.
- 22 Q. Chen and C. L. Hill, *Inorg. Chem.*, 1996, **35**, 2403.
- 23 Q. Chen, S. Liu and J. Zubietta, *Inorg. Chem.*, 1989, **28**, 4433.
- 24 D. N. Hendrickson, Y. S. Sohn and H. B. Gray, *Inorg. Chem.*, 1971, **10**, 1559.
- 25 D. Gatteschi, L. Pardi, A. I. Barra, A. Müller and J. Döring, *Nature (London)*, 1991, **354**, 463.
- 26 T. Yamase, *Polyoxometalates from Platonic Solids to Anti-retroviral Activity*, eds. M. T. Pope and A. Müller, Kluwer, Dordrecht, 1994, p. 337.

Received 10th February 1997; Paper 7/00916J